

Various multibody dynamic models for the description of plane Kirchhoff rods

Holger Lang[#], Hannah Laube[#], Sigrid Leyendecker[#]

[#] Chair of Applied Dynamics
University of Erlangen-Nuremberg
Haberstrasse 1, 91058 Erlangen, Germany
[holger.lang, hannah.laube, sigrid.leyendecker]@fau.de

Abstract

The plane Kirchhoff rod model is well known in continuum mechanics for the dynamic simulation of slender structures. It is a geometrically exact generalisation of the linear Euler-Bernoulli beam that takes into account extensional and bending deformations. In contrast to a Reissner rod [1], the rigid cross sections always stay perpendicular to the centerline of mass centroids [2]. Therefore, it does not incorporate transverse shear and is well suited for very slim structures.

We consider a Finite Element discretisation that is based on the discrete Kirchhoff beam kinematics displayed in Figure 1. It is a 2D restriction of the one proposed in [2, 3] for 3D Kirchhoff and Cosserat rods on a staggered grid. The proper choice of coordinates plays a crucial role concerning accuracy and numerical complexity during time integration. Here, we compare three approaches, which are well known in multibody dynamics simulations, and apply them to the proposed FE model.

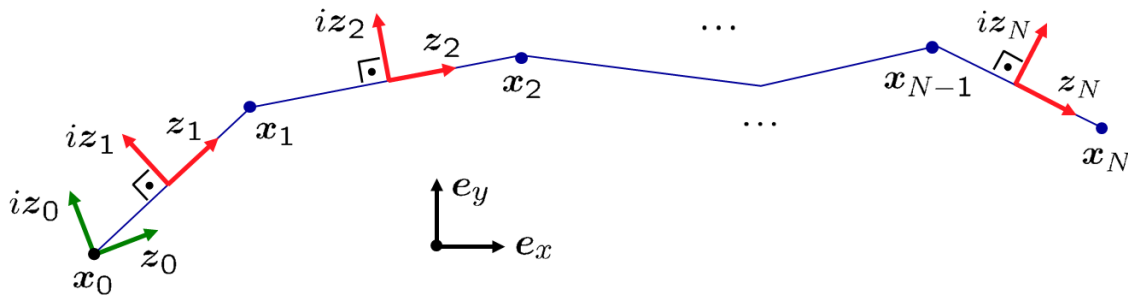


Figure 1: Plane Kirchhoff beam kinematics. The directors \mathbf{z}_n are parallel to the discrete centerline tangents $\mathbf{x}_n - \mathbf{x}_{n-1}$. The directors $i\mathbf{z}_n$ indicate the orientation of the cross section, perpendicular to the centerline tangents. The position \mathbf{x}_0 and orientation \mathbf{z}_0 are prescribed as boundary values.

The first approach uses *redundant absolute coordinates* $\mathbf{p} = (z_1, \mathbf{x}_1, \dots, z_N, \mathbf{x}_N)$, where the $\mathbf{x}_n \in \mathbb{R}^2$ stand for the absolute translations (i.e. the cross section centroids) and $\mathbf{z}_n \in \mathbb{S}^1 = \{\mathbf{z} \in \mathbb{C} : \|\mathbf{z}\|^2 = 1\} \simeq SO(2)$ for the absolute rotations (i.e. the cross section orientations). Complex numbers are used to enable the extension to a quaternionic formulation for 3D Kirchhoff beams later. The shear rigidity and the unity conditions for \mathbf{z}_n lead to internal holonomic constraints of the form $\mathbf{g}(\mathbf{p}) = \mathbf{0}$ with the d'Alembert constraint forces $\mathbf{G}(\mathbf{p})^\top \boldsymbol{\lambda}$, where $\mathbf{G}(\mathbf{p}) = \nabla \mathbf{g}(\mathbf{p})$. Then, the standard index 1 version of the equations of motion takes the form

$$\begin{bmatrix} \ddot{\mathbf{p}} \\ \boldsymbol{\lambda} \end{bmatrix} = \begin{bmatrix} \mathbf{M}(\mathbf{p}) & \mathbf{G}(\mathbf{p})^\top \\ \mathbf{G}(\mathbf{p}) & \mathbf{0} \end{bmatrix}^{-1} \begin{bmatrix} \mathbf{f}(\mathbf{p}, \dot{\mathbf{p}}, t) \\ -\dot{\mathbf{G}}(\mathbf{p}, \dot{\mathbf{p}})\dot{\mathbf{p}} \end{bmatrix} \quad (1)$$

with a state dependent mass $\mathbf{M}(\mathbf{p})$ and $\mathbf{f}(\mathbf{p}, \dot{\mathbf{p}}, t)$ incorporating the internal and external forces and moments. Due to the parametrisation of rotations by complex numbers, \mathbf{f} is free of trigonometric expressions and therefore fast to evaluate. Solving the linear system of equations in (1) in each time step grows with complexity $\mathcal{O}(N)$, as the structure is block-banded [4].

The second approach uses *minimal relative (or 'joint') coordinates* $\mathbf{q} = (w_1, \xi_1, \dots, w_N, \xi_N)$, where $\xi_n = \|\mathbf{x}_n - \mathbf{x}_{n-1}\|$ for the relative translations and $w_n = \Im(\bar{\mathbf{z}}_{n-1}\mathbf{z}_n)$ for the relative rotations. In the context of continuum mechanics, the magnitudes ξ_n correspond to the *extensional strains*, the w_n to the *bending curvatures*. This means that the strains are used as the primary unknowns instead of the displacements,

which is not standard. Let $\mathbf{q} = \boldsymbol{\psi}(\mathbf{p})$ resp. $\mathbf{p} = \boldsymbol{\varphi}(\mathbf{q})$ denote the forward resp. backward recursive coordinate transformation. System (1) is then transformed to the equivalent form

$$\mathbf{M}(\mathbf{q})\ddot{\mathbf{q}} = \boldsymbol{\Phi}(\mathbf{q})^\top \{ \mathbf{f}(\mathbf{p}, \dot{\mathbf{p}}, t) - \mathbf{M}(\mathbf{p})\dot{\boldsymbol{\Phi}}(\mathbf{q}, \dot{\mathbf{q}})\dot{\mathbf{q}} \}, \quad \mathbf{M}(\mathbf{q}) = \boldsymbol{\Phi}(\mathbf{q})^\top \mathbf{M}(\mathbf{p})\boldsymbol{\Phi}(\mathbf{q}), \quad (2)$$

where $\boldsymbol{\Phi}(\mathbf{q}) = \nabla \boldsymbol{\varphi}(\mathbf{q})$ and $\dot{\mathbf{p}} = \dot{\boldsymbol{\Phi}}(\mathbf{q})\dot{\mathbf{q}}$. By the use of BDF multistep methods, it is not necessary to solve (2) for $\ddot{\mathbf{q}}$. However, the effort in linear algebra grows like $\mathcal{O}(N^2)$, since the minimal mass $\mathbf{M}(\mathbf{q})$ is fully populated [4, 5].

The third approach is formulated in terms of *mixed coordinates*, as it is called in [5]. The system

$$\begin{bmatrix} \dot{\mathbf{p}} \\ \ddot{\mathbf{q}} \\ \boldsymbol{\lambda} \\ \boldsymbol{\eta} \end{bmatrix} = \begin{bmatrix} \mathbf{M}(\mathbf{p}) & \mathbf{0} & \mathbf{G}(\mathbf{p})^\top & -\boldsymbol{\Psi}(\mathbf{p})^\top \\ \mathbf{0} & \mathbf{0} & \mathbf{0} & \mathbf{E} \\ \mathbf{G}(\mathbf{p}) & \mathbf{0} & \mathbf{0} & \mathbf{0} \\ -\boldsymbol{\Psi}(\mathbf{p}) & \mathbf{E} & \mathbf{0} & \mathbf{0} \end{bmatrix}^{-1} \begin{bmatrix} \mathbf{f}(\mathbf{p}, \dot{\mathbf{p}}, t) \\ \mathbf{0} \\ -\dot{\mathbf{G}}(\mathbf{p}, \dot{\mathbf{p}})\dot{\mathbf{p}} \\ \boldsymbol{\Psi}(\mathbf{p}, \dot{\mathbf{p}})\dot{\mathbf{p}} \end{bmatrix}, \quad (3)$$

where $\boldsymbol{\Psi}(\mathbf{p}) = \nabla \boldsymbol{\psi}(\mathbf{p})$, is equivalent to (1), the analytic solution for the artificial Lagrange multiplier being $\boldsymbol{\eta} \equiv \mathbf{0}$. Solving the linear system of equations in (3) in each time step grows with complexity $\mathcal{O}(N)$, as the structure is block-banded [4]. However, the bandwidth is larger than the one in (1).

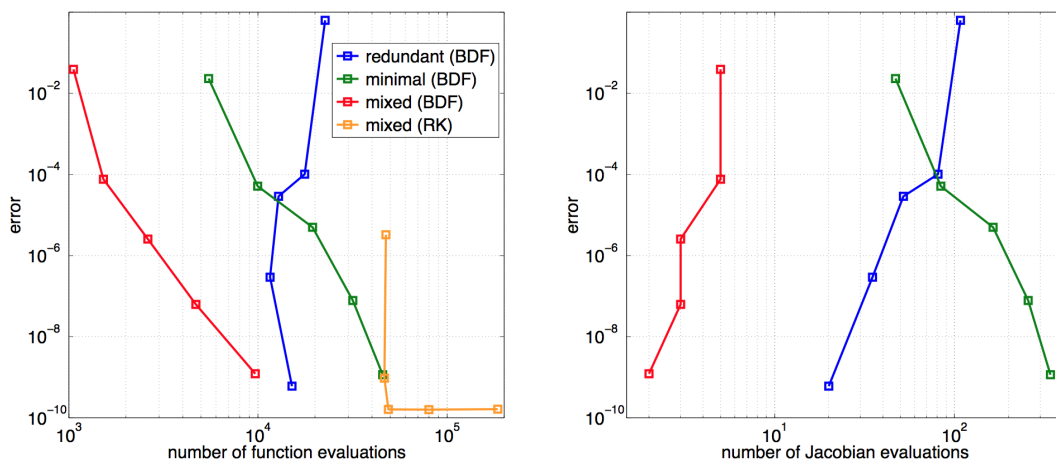


Figure 2: Numerical task in terms of right-hand-side function evaluations (left) and Jacobian evaluations (right) for a Kirchhoff rod with $N = 25$ elements and a rubber-like material.

The discussion of pros and cons for each of the formulations (1), (2) and (3) with respect to numerical effort (e.g. function calls and time step sizes) and accuracy is part of the work. As an example, Figure 2 displays some statistical results that are typical in conjunction with the MATLAB time integrators ODE15S, a BDF multistep method, and ODE45, an explicit Runge-Kutta method based on the scheme of Dormand and Prince [6].

References

- [1] J.C. Simo. A finite strain beam formulation: the three dimensional dynamic problem – Part I. Computer Methods in Applied Mechanics and Engineering, Vol. 49, No. 3, pp. 55–70, 1985.
- [2] H. Lang, M. Arnold. Numerical aspects in the dynamic simulation of geometrically exact rods. Applied Numerical Mathematics, Vol. 62, No. 3, pp. 1411–1427, 2012.
- [3] H. Lang, J. Linn, M. Arnold. Multibody dynamics simulation of geometrically exact Cosserat Rods. Multibody System Dynamics, Vol. 25, No. 3, pp. 285–311, 2012.
- [4] G. Golub, C. Van Loan. Matrix computations. Third edition, John Hopkins university press, 1996.
- [5] E. Eich-Soellner, C. Führer. Numerical methods in multibody dynamics. Teubner, 1998.
- [6] L.F. Shampine, M.W. Reichelt. The Matlab ODE suite. SIAM Journal on Scientific Computing, Vol. 18, No. 1, pp. 1–22, 1997.